Electronic Supporting Information

Aggregation-Induced Emission (AIE) Organic Metal Halide Complex for X-ray Scintillation

Tunde Blessed Shonde,[a] He Liu,[a] Oluwadara Joshua Olasupo,[a] Alexander Bouchard,[a] Sara Bouchard,[a] Annaliese Franklin,[a] Xinsong Lin,[a] Luis M. Stand,[c,d] Biwu Ma *[,a,b]

[a] Department of Chemistry and Biochemistry, Florida State University, Tallahassee, FL, 32306, USA.
[b] Materials Science and Engineering Program, Florida State University, Tallahassee, FL 32306, USA
[c] Department of Nuclear Engineering, University of Tennessee, Knoxville, TN 37996, USA.
[d] Scintillation Materials Research Canter, University of Tennessee, Knoxville, TN 37996, USA.
*Email: bma@fsu.edu

Experimental Section

Materials: Zinc Chloride (99.999%), 4-bromotriphenylamine (97%), pyridine-4-boronic acid (90%), tetrakis(triphenylphosphine)-palladium(0),(99%), potassium carbonate (≥99.0%), tetrahydrofuran (THF, ≥99.9%), methanol (MeOH, ≥99.9%), dichloromethane (DCM, ≥99.8%), poly methylmethacylate (average molecular weight- 120, 000) were all purchased from Sigma Aldrich. N, N-Dimethylformamide (DMF ≥99.8%), and diethyl ether (Et_2O, ≥99.9%) were purchased from VWR. These materials were used without further purification after purchase. The elemental analysis was performed by Atlantic Microlab, Inc., Norcross, Georgia, USA.

Synthesis of N, N-diphenyl-4-(pyridin-4-yl) aniline (TPA-PD): 4-Bromotriphenylamine (7.4 mmol, 324.21 g/mol, 2.4 g), pyridine-4-boronic acid (12 mmol, 122.92 g/mol, 1.475 g), tetrakis(triphenylphosphine)-palladium(0) (0.297 mmol, 1155 g/mol, 0.344 g) and potassium carbonate (14.4 mmol, 138.21 g/mol, 2 g) were weighed into clean flask. This was followed by three cycles of repeated purging with N_2 and vacuum evacuation. A 120 ml of combined solvent (THF: MeOH; 1:1) of THF and MeOH was added with two cycles of purging with N_2 and vacuum evacuation. The mixture was refluxed at 90 ^oC for 36 hours under an N_2 atmosphere and then concentrated by rotary evaporation. TPA-PD was purified by column chromatography on silica gel with a mixture of petroleum ether and ethyl acetate as the eluent (7:1 by volume) to obtain about 55% TPA-PD white solid yield after recrystallization with DCM. ^1H NMR (600 MHz, DMF-D7) δ 8.65 - 8.61 (m, 2H), 7.82 (d, J = 8.7 Hz, 2H), 7.75 - 7.71 (m, 2H), 7.44 - 7.37 (m, 4H), 7.19 - 7.13 (m, 6H), 7.11 (d, J = 8.7 Hz, 2H).; HRMS (ESI) m/z: calc. value: 322.15; found 323.1567. Elemental analysis for TPA-PD ($C_{23}H_{18}N_2$) calculated: C, 85.68; H,5.63; N, 8.69. Found C, 84.86; H, 5.58; N, 8.69.

Synthesis of N,N-diphenyl-4-(pyridine-4-yl)aniline zinc (II) chloride $(TPA\text{-}PD)_2ZnCl_2$): 2:1 molar ratio of N,N-diphenyl-4-(pyridine-4-yl)aniline and zinc chloride were fully dissolved in the appropriate amount of DMF to form a precursor solution. This was followed by the addition of acetonitrile, 3× the volume of the precursor solution. Crystal formation of $(TPA\text{-}PD)_2ZnCl_2$) within a few hours to a day is observed. This is followed by

washing with Et_2O, achieving about 87% yield of $(TPA\text{-}P)_2ZnCl_2$. ^1H NMR (600 MHz, DMF-D7) δ 8.69 – 8.65 (m, 2H), 7.90 – 7.84 (m, 4H), 7.41 (dd, J = 8.4, 7.5 Hz, 4H), 7.17 (ddd, J = 3.7, 3.0, 1.3 Hz, 6H), 7.11 (d, J = 8.8 Hz, 2H). Elemental analysis for $(TPA\text{-}PD)_2ZnCl_2$ ($C_{46}H_{36}N_4ZnCl_2$); Calculated: C, 70.73; H, 4.65; N, 7.17; Cl, 9.08. Found: C, 70.50; H, 4.65; N, 7.42; Cl, 9.09.

Fabrication of X-ray imaging scintillator film: 120 mg of $(TPA\text{-}PD)_2ZnCl_2$ crystals were initially partially dissolved in 0.5 ml of chloroform. To ensure thorough mixing, the solution was vortex-mixed and sonicated for 2 hours. Following the dissolution of the crystals, 80 mg of poly(methyl methacrylate) (PMMA) was added to the solution. This mixture was then subjected to an additional 2 hours of sonication. Once this step was complete, the resulting solution was further stirred using a magnetic stirrer for 30 minutes. To prepare the substrate for film deposition, an ozone-cleaned glass surface was utilized. The well-mixed and homogenized slurry was carefully drop-cast onto the glass substrate and allowed to dry for 24 hours. It is noteworthy that during the drying process, a beaker housing was used to cover the substrate. This precaution was taken to ensure the film's uniformity and quality.

Structural Characterization

Single-crystal X-ray data for $(TPA\text{-}P)_2ZnCl_2$ was collected using a Rigaku XtaLAB Synergy-S diffractometer equipped with a HyPix-6000HE Hybrid Photon Counting (HPC) detector and dual Mo and Cu microfocus sealed X-ray source at 150 K. The powder X-ray diffraction (XRD) patterns were obtained using a Rigaku Smartlab powder diffractometer equipped with a Cu Kα X-ray source. Diffraction patterns were recorded from 5° to 50° 2θ with a step size of 0.05° under a tube current of 44 mA and tube voltage of 40 kV at room temperature. Further structural analysis of TPA-PD was done using ^1H B500 NMR equipped with a high-resolution 5 mm TXI (H-C/N-D) Zg probe. Mass spectrometry was performed using liquid chromatography- time-of-flight/mass spectrometry (LC-TOF/MS) (TOF 6230, LC 1260, Agilent) in a positive electrospray ionization (ESI) mode with a mass range of 100 – 1700 m/z.

Optical Characterization

Excitation and steady-state photoluminescence were carried out using an Edinburgh FS5 steady state spectrometer with a 150 W xenon lamp. Time-Correlated Single Photon Counting (TCSPC) was performed for 10,000 counts using excitation from an Edinburgh EPL-360 picosecond pulsed diode laser. The PL decay was fitted using a biexponential decay function for TPA-PD and $(TPA\text{-}PD)_2ZnCl_2$ and a mono-exponential decay function for BBPZn. The weighted average lifetime was computed according to equation (1).

$$\tau_{avg} = \frac{\sum \alpha_i \tau_i^2}{\sum \alpha_i \tau_i} \quad \text{.....(1)}$$

where τ_i represents the decay time, and α_i represents the amplitude of each component. PLQY measurement was performed using Hamamatsu Quantaurus-QY Spectrometer (Model C11347-11) equipped with a xenon lamp, an integrating sphere sample chamber, and a CCD detector. The PLQYs were calculated using the equation;

$$\eta QE = \frac{I_s}{ES_R - ES_s} \quad \text{.....(2)}$$

Where I_s stands for the photoluminescence emission spectrum of the sample, and ES_S and ES_R represent the excitation spectrum for the sample and reference, respectively.

Thermal Stability Analysis

DSC studies were done using a TA instrument Q600 system. The sample was heated from room temperature to 700 °C at a 5 °C/min rate under an argon flux of 100 mL/min.

Radioluminescence Spectrum

The RL spectra were acquired using an Edinburgh FS5 spectrofluorometer (Edinburgh Instruments) equipped with an X-ray source (Moxtek Mini-X tube with a W target and 4 W maximum power output, see Table S5 for voltage, current X-ray dose relationship). The X-ray response intensity was examined and collected by a Hamamatsu R928 PMT. The radiation dose rate of the X-ray source was calibrated by using RaySafe 452 dosimeter. The pulse height spectra of ^{137}Cs were collected using a standard bialkali Hamamatsu R2059 photomultiplier tube connected to a Canberra 2005 pre-amplifier, Ortec 672 spectroscopy amplifier, and a Tukan 8K multichannel analyzer. A shaping time of 10 μs was used to ensure complete light collection. The absolute light yield in photons per MeV was measured via the single photoelectron technique using a factory-measured quantum efficiency R2059 PMT.

To determine the Limit of detection (LOD), a series of the background signals were recorded without the sample under X-ray irradiation under 3.08 to 221.39 to 3.08 $\mu Gy\ s^{-1}$ measurement. Then, a series of signal responses were taken with the sample under the above conditions, and the slope was determined. The LOD was calculated using the equation below, where Bk_{std} is the standard deviation of the background responses.

$$LOD = \frac{3 * Bk_{std}}{Slope} \quad \text{.....(5)}^{1}$$

X-ray imaging

The X-ray imaging system is a lab-built X-ray imaging system comprising of an X-ray, sample holder, light ray reflector, and a digital camera. The X-ray source used in the imaging was a Moxtek Mini-X tube with a W target and 4 W maximum power output. In this built imaging system, the X-ray beam passed vertically through the object of interest, and the scintillator film, right below it. The optical path of resulting radioluminescence was then deflected towards the camera by a reflector angled at the imaging system to remove the negative effect caused by direct X-ray irradiation of the camera. A digital camera was used to capture the deflected image and save it in jpeg format.

Table S1. Single crystal structure data of $(TPA\text{-}PD)_2ZnCl_2$

	$(TPA\text{-}PD)_2ZnCl_2$
Compound	$(C_{23}H_{18}N_2)_2ZnCl_2$
CCDC number	2181767
Empirical formula	$C_{46}H_{36}N_4ZnCl_2$
Molecular weight/g/mole	781.06
Temperature/K	150
Crystal system	Monoclinic
Space group	$P2_1/c$
a/Å	21.9901(3)
b/Å	11.7699(2)
c/Å	15.3428(2)
α/°	90
β/°	106.6460(2)
γ/°	90
Volume/Å^3	3804.63(12)
Z	4
P_{calc} g/cm^3	1.364
F (000)	1616.0
H_{max}, k_{max}, l_{max}	27,14,19
T_{min}, T_{max}	0.059,0.620
μ/mm^{-1}	2.483
R_1, wR_2	0.0487[a], 0.1378[b]
Goodness-of-fit on F^2	1.085

a)$R_1 = \sum||Fo|-|Fc||/\sum|Fo||$. b) $wR_2 = [\sum w(Fo^2 - Fc^2)^2 / \sum w(Fo^2)^2]^{1/2}$

Table S2. Selected bond distance and angles of $(TPA\text{-}PD)_2ZnCl_2$.

Bonds	**Angle (°)**
Cl_1-Zn_1-Cl_2	122.19
Cl_1-Zn-N_1	107.23
Cl_1-Zn_1-N_3	105.50
Cl_2-Zn_1-N_1	107.99
N_1-Zn_1-N_3	104.33
Zn1-N1-C_{24}	121.2
Zn_1-N_1-C_{28}	120.1
Bonds	**Distance (Å)**
Zn_1-Cl_1	2.23
Zn_1-Cl_2	2.24
Zn1-N1	2.05
Zn_1-N_3	2.04

Table S3. Fitting parameters for PL decay kinetics of BBPZn, TPA-PD, and $(TPA\text{-}PD)_2ZnCl_2$.

	A_1	**τ_1 (ns)**	**A_2**	**τ_2 (ns)**	**τ_{avg} (ns)**

BBPZn	1.0000	4.0036			4.00
TPA-PD	0.6816	0.9657	0.3184	2.9245	1.59
$(TPA\text{-}PD)_2ZnCl_2$	0.8388	1.1588	0.1612	4.1841	1.81

Table S4. A figure of merit for reported scintillators based on metal-organic complexes.

S/N	**Material**	**Light yield (Photon/MeV)**	**Decay lifetime (ns)**	**LOD ($nGyS^{-1}$)**	**Ref**
1	CP1	21037	8.47×10^6 (PL)	34.45	[1]
2	CP2	10580	4.36×10^6 (PL)	62.64	[1]
3	CP3	13470	2.31×10^6 (PL)	45.02	[1]
4	$(DXP)_2MnBr$	18 400	8.01×10^6 (PL)	65.1	[2]
5	Tb-TPC	5453	1.34×10^5 (PL)	1114	[3]
6	Eu-TPC	6121	4.63×10^5 (PL)	520	[3]
7	$CeCl_3$-Bu	1920	NA	NA	[4]
8	$CeBr_3$-Prop	3218	NA	NA	[4]
9	Tb-1	4800	7.64×10^5 (PL)	243	[5]
10	Passivated -Tb-1	9000	NA	146	[5]
12	BBPZn	6249	4.00 (PL) 6.78 (RL)	15.56	This work
13	$(TPA\text{-}PD)_2ZnCl_2$	13 423	1.81 (PL) 5.24 (RL)	80.23	This work

Table S5. Experimental dose rate.

S/N	**Dose rate (µgray/sec)**	**Voltage (kV)**	**Current (µA)**
1	221.39	40	100

2	210.56	40	95
3	199.44	40	90
4	188.06	40	85
5	177.22	40	80
6	166.11	40	75
7	155.00	40	70
8	143.89	40	65
9	132.78	40	60
10	121.67	40	55
11	110.83	40	50
12	99.72	40	45
13	88.61	40	40
14	77.5	40	35
15	66.38	40	30
16	55.28	40	25
17	44.17	40	20
18	31.39	35	20
19	19.14	30	20
20	9.03	25	20
21	3.08	20	20

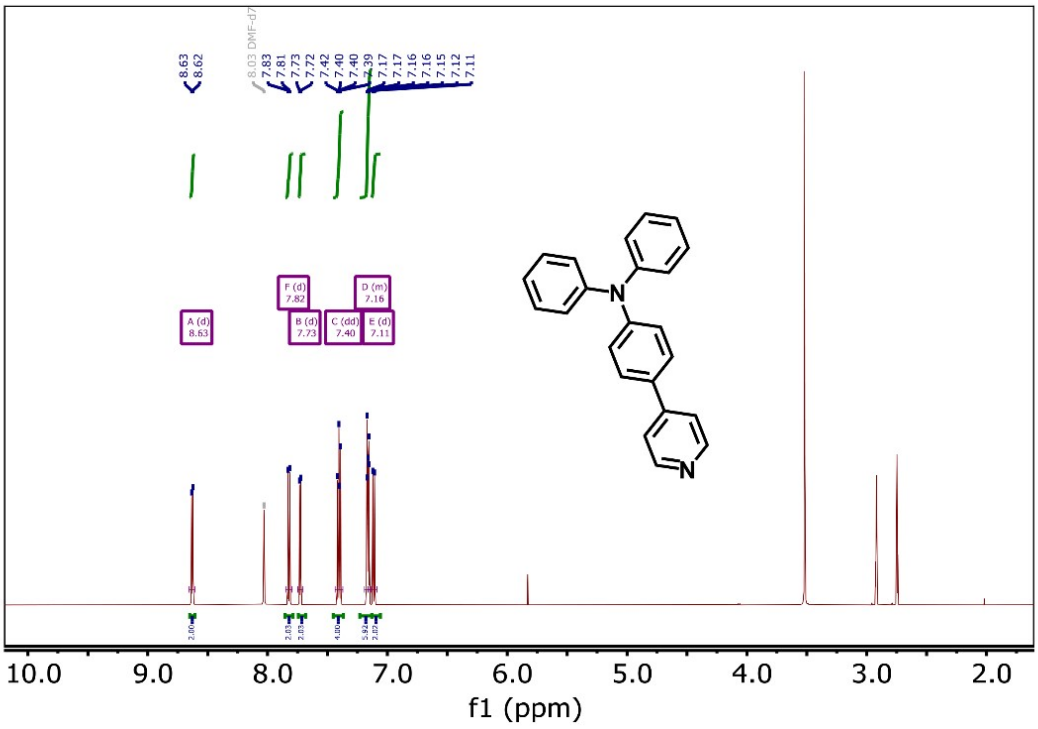

Figure S1. NMR characterization of TPA-PD. ^{1}H NMR of TPA-PD.

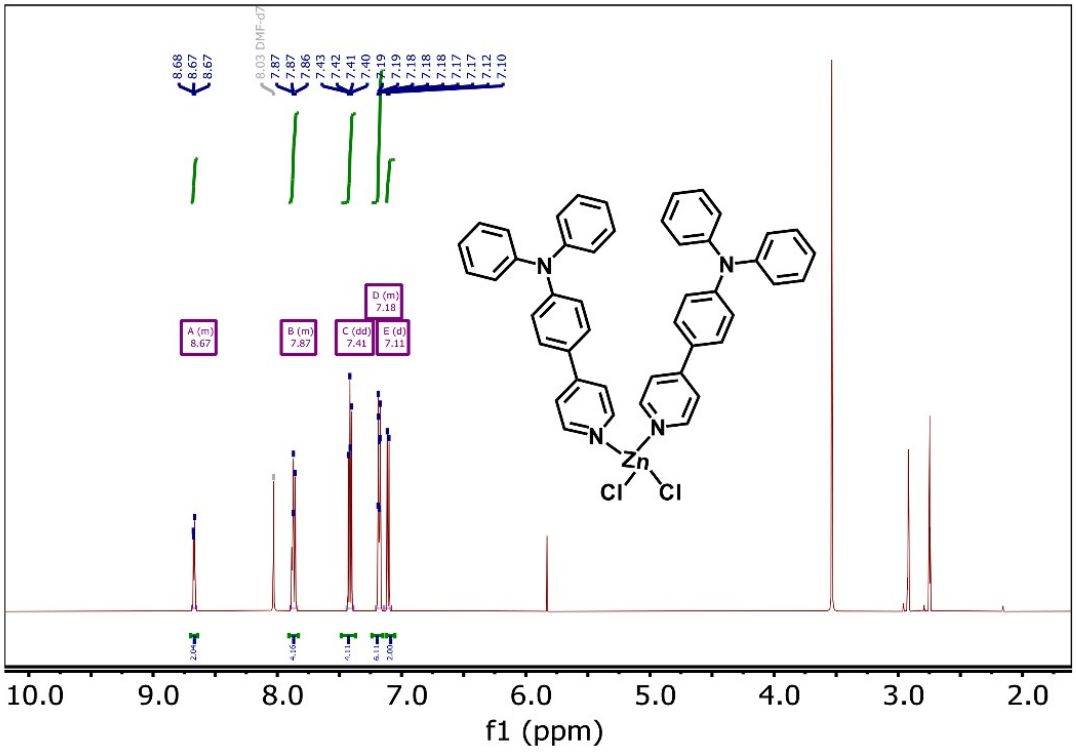

Figure S2. NMR characterization of $(TPA\text{-}PD)_2ZnCl_2$. ^{1}H NMR of $(TPA\text{-}PD)_2ZnCl_2$.

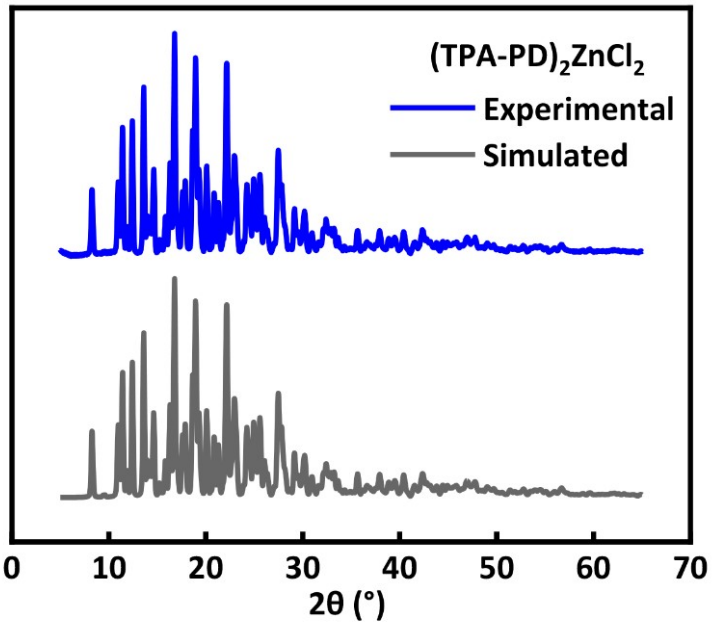

Figure S3. PXRD of $(TPA\text{-}PD)_2ZnCl_2$. Comparison between the experimental and simulated PXRD Patterns of $(TPA\text{-}PD)_2ZnCl_2$.

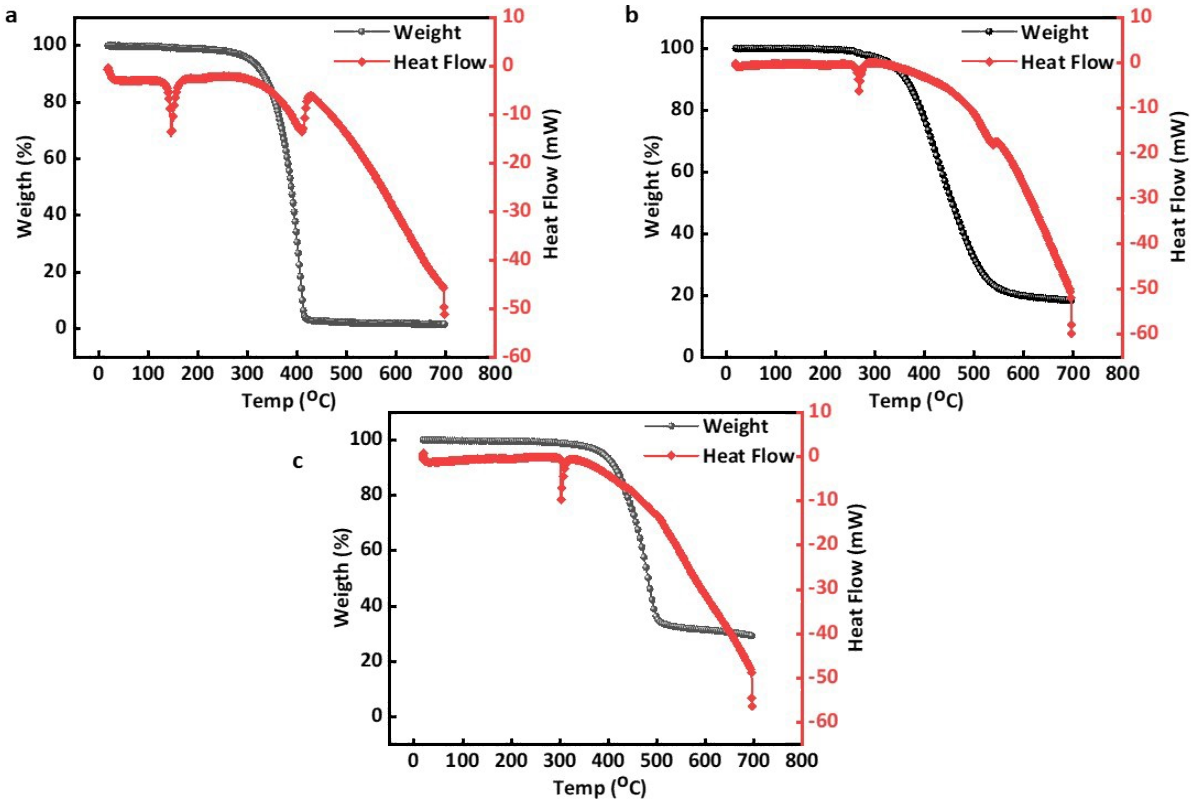

Figure S4. Thermal analysis. Thermogravimetric and differential scanning calorimetric analysis of a) TPA-PD; b) $(TPA\text{-}PD)_2ZnCl_2$; (c) BBPZn.

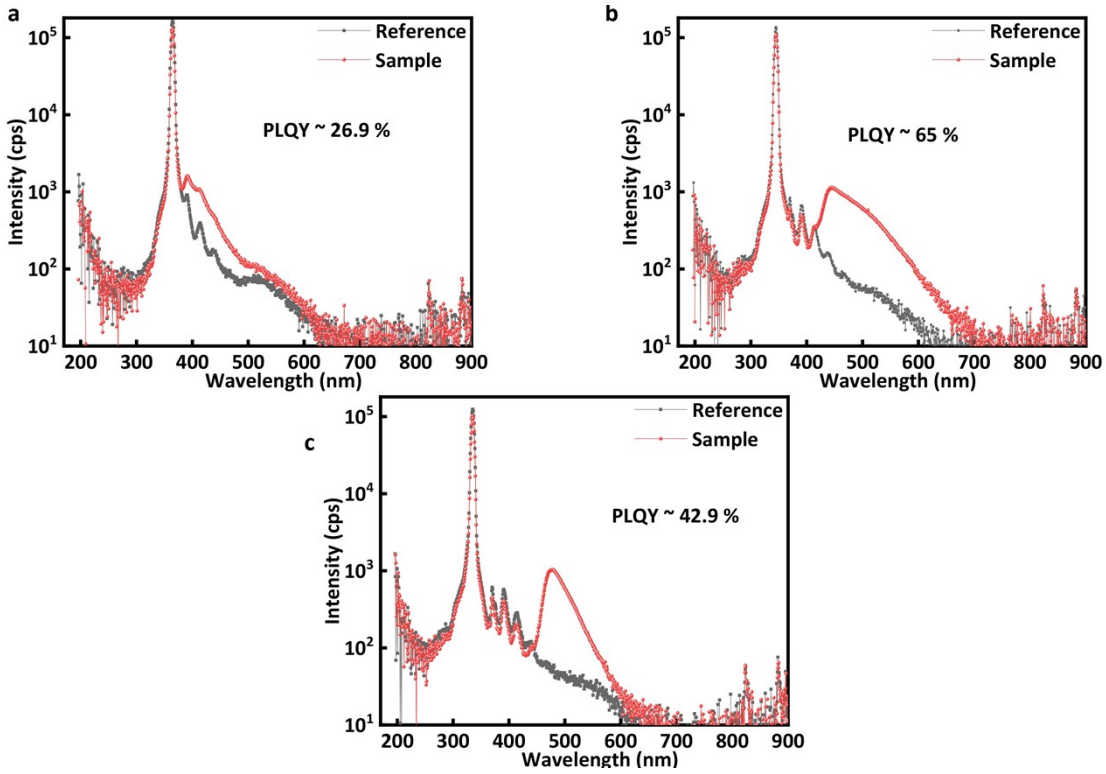

Figure S5. Photophysical Characterization. Photoluminescence Quantum Yields of; (a)TPA-PD; (b) (TPA-PD)$_2$ZnCl$_2$; and (c) BBPZn.

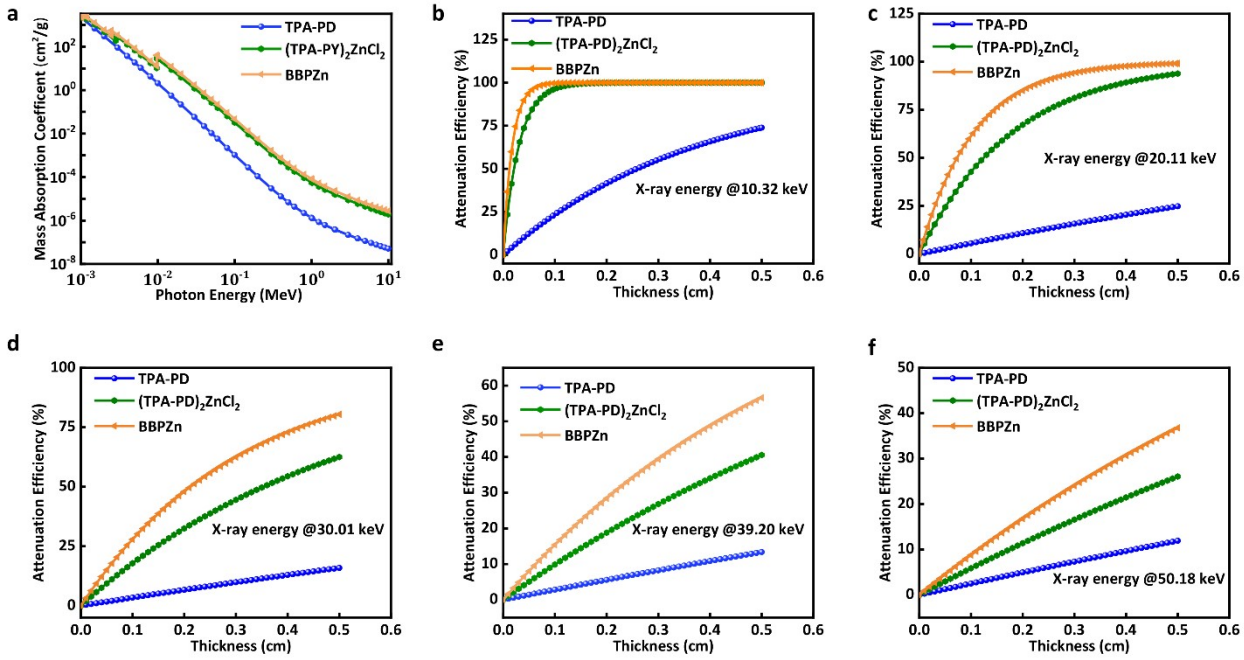

Figure S6. Computed high-energy radiation absorption. (a) Mass absorption coefficient vs photon energy plot of TPA-PD, (TPA-PD)$_2$ZnCl$_2$ and BBPZn; (b, c, d, e) X-ray Energy (10.32 KeV, 20.11 KeV, 30.01 keV, 39.20 keV and 50.18 keV respectively) efficiency vs thickness of TPA-PD, (TPA-PD)$_2$ZnCl$_2$, and BBPZn.

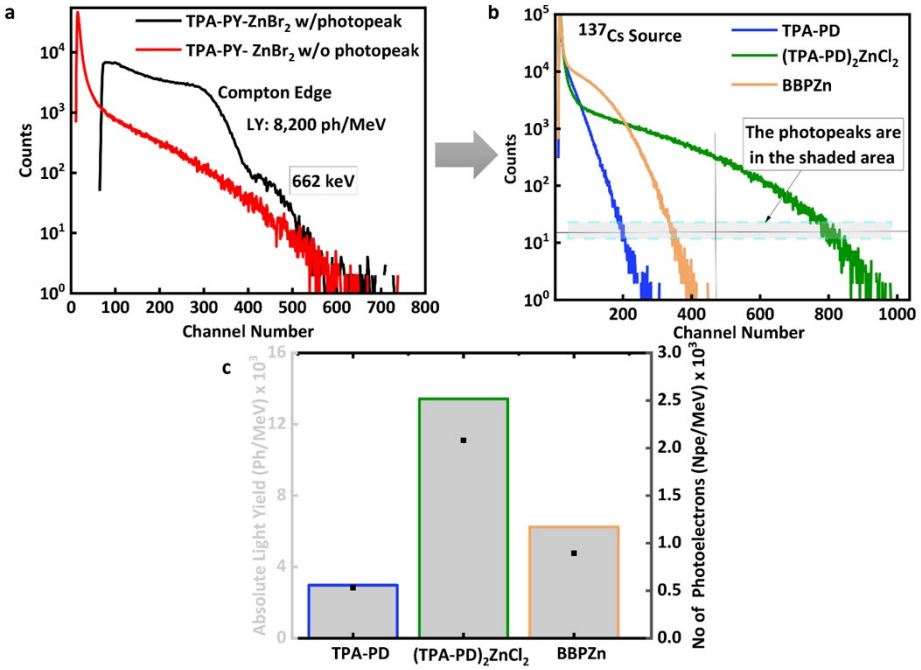

Figure S7. Absolute light yield measurement. (a) Counts vs Channel plot of $(TPA\text{-}PD)_2ZnBr_2$ with ^{137} Cs excitation source (b)Counts vs Channel plot of TPA-PD, $(TPA\text{-}PD)_2ZnCl_2$ and BBPZn with ^{137} Cs excitation source; (c) Absolute light and number of photoelectrons bar chart of TPA-PD, $(TPA\text{-}PD)_2ZnCl_2$, and BBPZn.

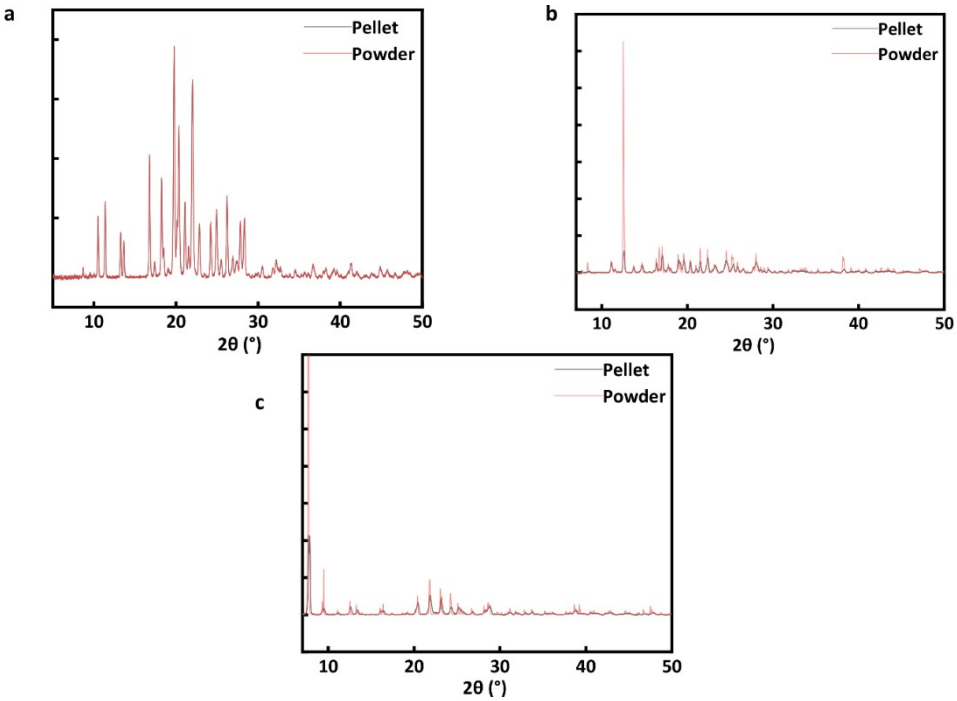

Figure S8. Powder X-ray Diffraction (PXRD). PXRD data comparison of pellet and powder of (a) TPA-PD; (b) $(TPA\text{-}PD)_2ZnCl_2$; (c) BBPZn.

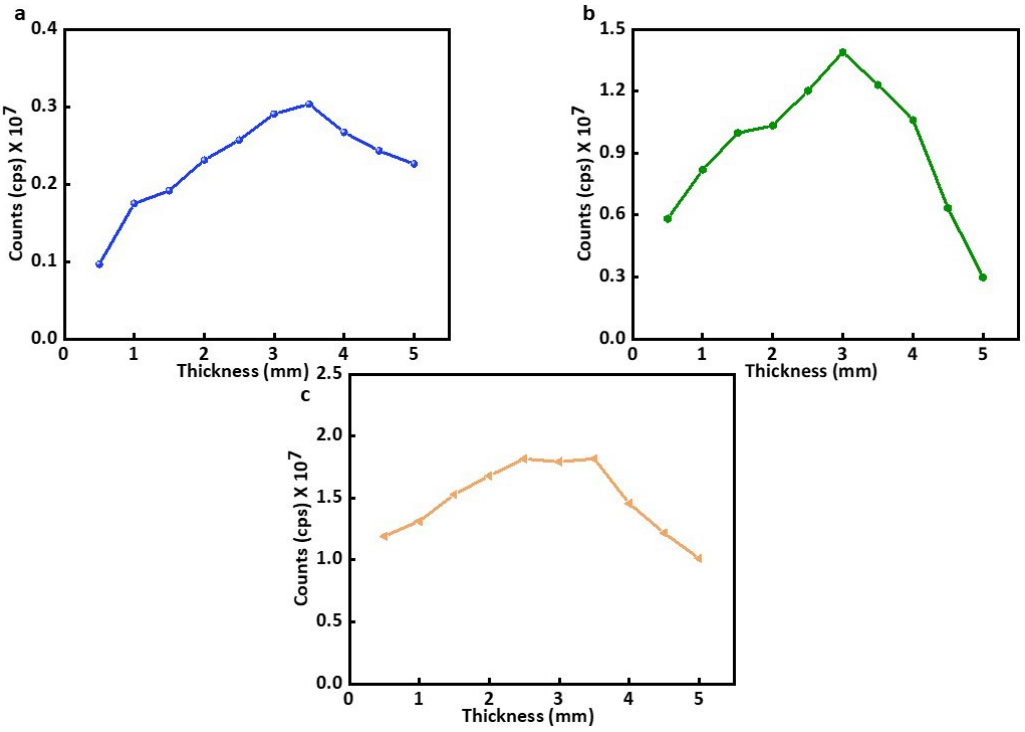

Figure S9. Thickness-dependent radioluminescence. Integrated radioluminescence of (a) TPA-PD; (b) $(TPA\text{-}PD)_2ZnCl_2$; (c) BBPZn at different thicknesses.

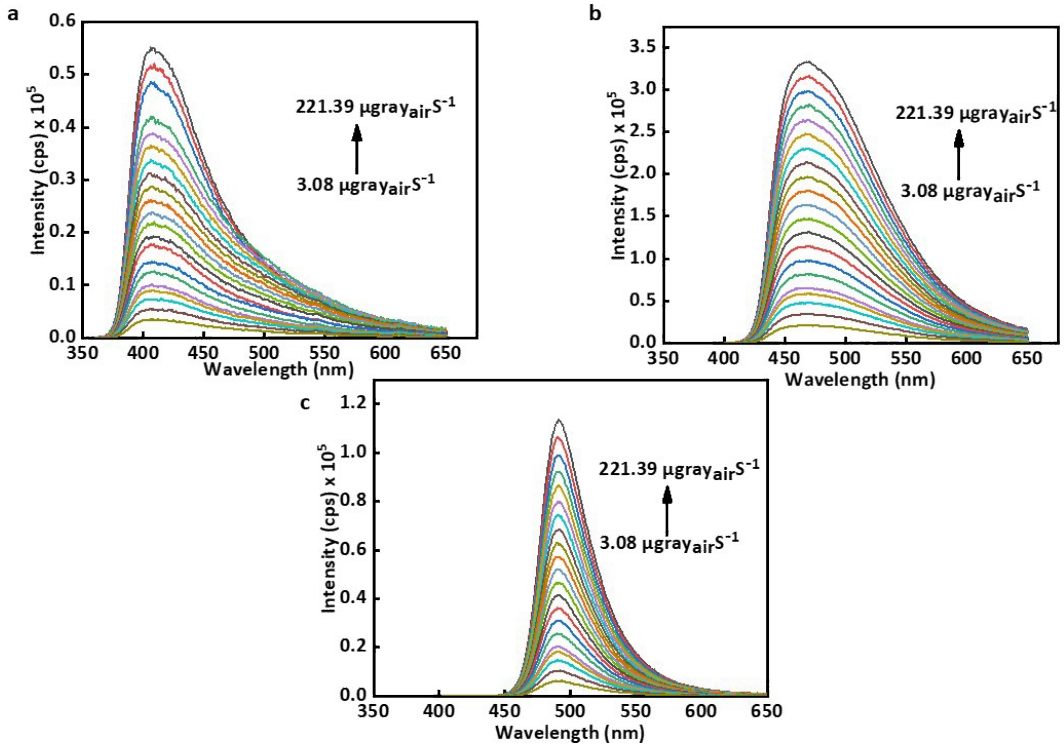

Figure S10. Dose-Response. Radioluminescence spectra of under X-ray excitation dose rate from 221.39 to 3.08 $\mu Gy_{air}\ s^{-1}$ of; (a)TPA-PD; (b) $(TPA\text{-}PD)_2ZnCl_2$; (c) BBPZn.

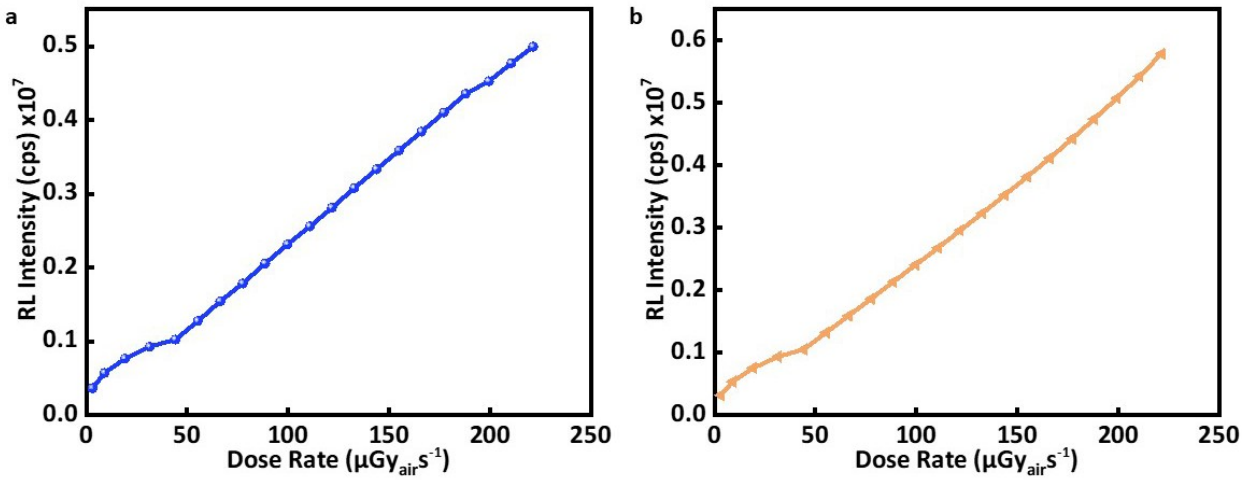

Figure S11. Dose-Response. Integrated radioluminescence spectra under X-ray excitation dose rate from 221.39 to 3. 08 $\mu Gy_{air}\ s^{-1}$ of; (a)TPA-PD; (b) BBPZn.

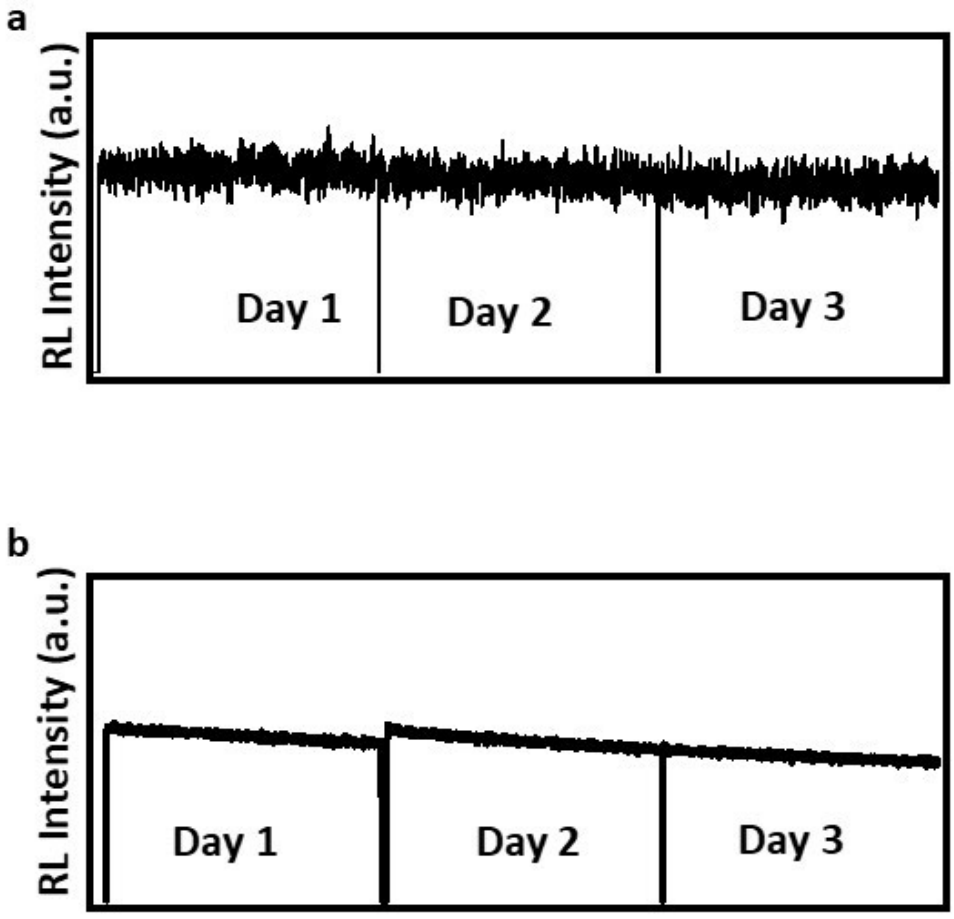

Figure S12. Radio-stability. Radiation stability under continuous irradiation (221.39 $\mu Gy_{air}\ s^{-1}$) for 30 mins for Day 1, Day 2 and Day 3 of; (a) TPA-PD; (b) BBPZn.

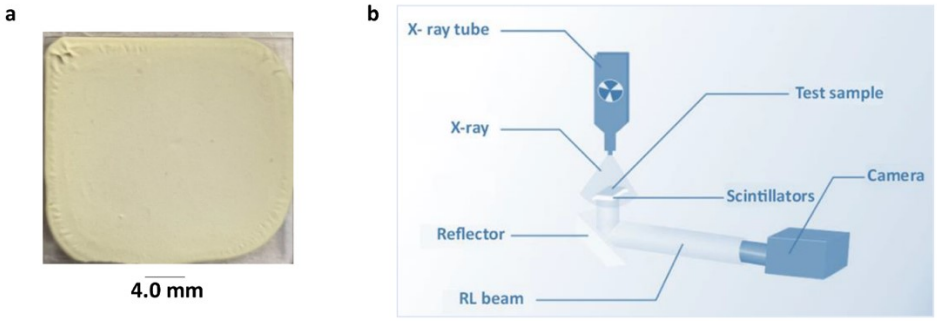

Figure S13. (a) 60 wt% $(TPA\text{-}PD)_2ZnCl_2$ - PMMA composite; (b) Schematic of lab-built X-ray imaging setup.

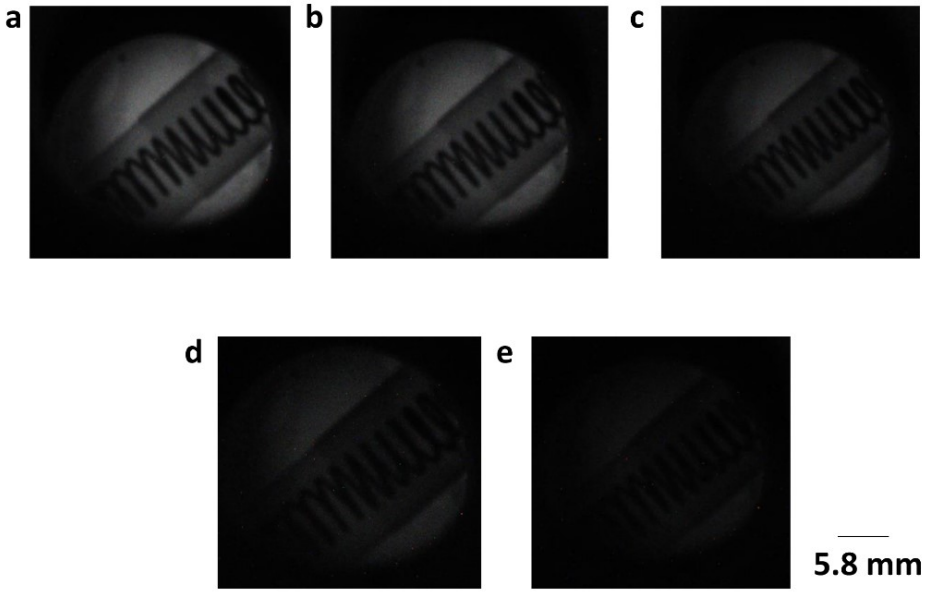

Figure S14. X-ray Images of encapsulated spring under various X-ray dose rates. X-ray images under; (a) 40 kV. 100µA; (b) 40 kV, 60 µA; (c) 40 kV, 40 µA; (d) 20 kV, 100µA; (e) 40 kV, 20 µA X-ray irradiation

References

1. Z. Zhou, H. Meng, F. Li, T. Jiang, Y. Yang, S. Liu and Q. Zhao, *Inorg Chem*, 2023, **62**, 5729-5736.
2. H. Meng, W. Zhu, F. Li, X. Huang, Y. Qin, S. Liu, Y. Yang, W. Huang and Q. Zhao, *Laser & Photonics Reviews*, 2021, **15**, 2100309.
3. X. Liu, S. Wang, W. Xie, J. Ni, K. Xiao, S. Liu, W. Lv and Q. Zhao, *Journal of Materials Chemistry C*, 2023, **11**, 7405-7410.
4. L. A. Boatner, J. S. Neal, J. O. Ramey, B. C. Chakoumakos, R. Custelcean, E. V. D. Van Loef, G. Markosyan and K. S. Shah, *Nuclear Instruments and Methods in Physics Research Section A: Accelerators, Spectrometers, Detectors and Associated Equipment*, 2013, **703**, 138-144.
5. Z. Chen, D. Lu, H. Xie, X. Yang, Y. Li, C. Bao, L. Lei and S. Xu, *Advanced Optical Materials*, 2021, **10**, 2102074.